Birth and early evolution of a planetary nebula

Matthew Bobrowsky*, **Kailash C. Sahu**†, **M. Parthasarathy**‡
& Pedro García-Lario§

* *Orbital Sciences Corporation, 7500 Greenway Center Drive, No. 700, Greenbelt, Maryland 20770, USA*
† *Space Telescope Science Institute, 3700 San Martin Drive, Baltimore, Maryland 21218, USA*
‡ *Indian Institute of Astrophysics, Koramangala, Bangalore 560034, India*
§ *ISO Science Operations Centre, Villafranca del Castillo, Apartado de Correos 50727, 28080 Madrid, Spain*

The final expulsion of gas by a star as it forms a planetary nebula—the ionized shell of gas often observed surrounding a young white dwarf—is one of the most poorly understood stages of stellar evolution[1,2]. Such nebulae form extremely rapidly (about 100 years for the ionization) and so the formation process is inherently difficult to observe. Particularly puzzling is how a spherical star can produce a highly asymmetric nebula with collimated outflows. Here we report optical observations of the Stingray nebula[3,4], which has become an ionized planetary nebula within the past few decades[5]. We find that the collimated outflows are already evident, and we have identified the nebular structure that focuses the outflows. We have also found a companion star, reinforcing previous suspicions that binary companions play an important role in shaping planetary nebulae and changing the direction of successive outflows[6].

Our narrow-band images (Fig. 1) show the compact nebula—which we refer to as the 'Stingray nebula'—that surrounds the central star of He3-1357 (also known as CPD-59°6926, SAO244567 and IRAS17119-5926). In most of the images, the emission appears most strongly concentrated in an ellipse with its major axis subtending 1.6″ from northeast to southwest. (This represents a correction from the orientation that we published previously[7].) If the ellipse is actually a circular ring viewed obliquely, then our line of sight is inclined from the actual axis of symmetry by 56°. Above and below the ring are bubbles that are blown open at the poles. In earlier images from the Wide Field and Planetary Camera 1 (WFPC1)—obtained before the spherical aberration of the Hubble Space Telescope was corrected—gas could just barely be seen escaping from these bubbles[7]. However, in the new WFPC2 images that we present here, the superior spatial resolution allows us to see that the escaping gas forms a complex system of collimated outflows. (The nomenclature used for the various nebular features is shown in Fig. 2.) In addition, the higher signal-to-noise ratio of the new images reveals that emission extends in all directions well outside the main bubble and ring structures. This is particularly evident in the low-ionization images. In three of these images—[O I] (shown in Fig. 1), [N II] and [S II] (not shown, but similar to [O I])—the ring is much fainter and more mottled than in the other images. In most of the images (including the continuum image), the equatorial ring has dimensions 1.67″ × 0.92″. But in the [O I], [N II] and [S II] images, the minor axis is slightly longer, 1.0″, presenting a visibly larger eccentricity of 0.83 rather than 0.79 in the case of the other images. In these same three images, the southeastern inner collimated outflow appears to be two separate, but closely situated, collimated outflows. The overall shape of the nebula evokes the name 'Stingray nebula'.

The mass outflow that we observe is consistent with the blue-shifted Si IV (1,394–1,403 Å), C IV (1,548–1,551 Å) and Al III (1,855–1,863 Å) doublets that indicated the presence of a strong stellar wind[5]. The low-ionization images show the strongest nebular emission coming from the collimated outflows close to the holes in the bubbles where gas is escaping. This is consistent with shock

excitation caused by the wind encountering the shell and being focused by it. Although converging flows have been observed previously[8], and hydrodynamic models have been used to simulate the formation of collimated outflows for almost two decades[9–14], this is the first observation that clearly shows the collimating mechanism of bipolar outflows. Although theoretical work on bipolar outflows has often involved asymmetrical mass loss due to rapid stellar rotation or a toroidal magnetic field, or the presence of disks (accretion disks or protostellar disks) to collimate the outflows, the latter process is not the mechanism observed in the Stingray nebula. The outflows in the Stingray are focused by the nebular bubbles which function like nozzles, with the gas leaving through the polar holes. Bipolar structures have been seen both in protoplanetary nebulae (PPN) and in planetary nebulae (PN), but this is the only object that has been followed spectroscopically from its pre-ionized PPN stage[3,4] through ionization and recognition as a PN[5]. So it is especially interesting that the collimating mechanism is
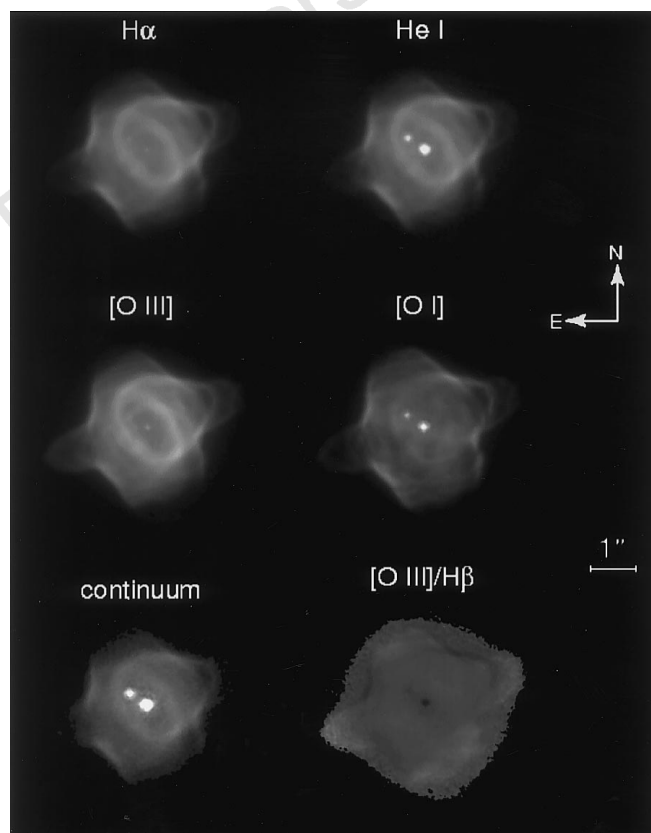

Figure 1 Hubble Space Telescope narrow-band images of He3-1357, the Stingray nebula. The images were obtained in four emission lines (Hα, He I 5,876-Å, [O I] 6,300-Å and [O III] 5,007-Å), a continuum range of the spectrum centred at 6,193 Å, and the ratio of [O III] 5,007 Å to Hβ. Observations were made in March 1996 with WFPC2 using the narrow-band filters F487N, F502N, F588N, F630N and F656N. The continuum exposure was made using filter FQCH4N15 which has a passband of ~44 Å centred at 6,193 Å. Although not shown in this figure, images were also acquired with filters F658N ([N II] 6,583-Å) and F673N ([S II] 6,731-Å) which show the nebula with an appearance almost identical to the [O I] image shown here. The routine scientific data processing included bias, preflash, dark, and flat-field corrections. After removing bad pixels resulting from cosmic rays, both images from the same filter were aligned and averaged. The ratio of the [O III] 5,007-Å to Hβ emission (bottom right panel) varies across the nebula. Relative to Hβ, the [O III] emission is lowest ([O III]/Hβ ≈ 2) near the central star, and is also low ([O III]/Hβ ≈ 4) in the denser regions of the bubbles where the gas has been most compressed. The low [O III]/Hβ ratio in these areas is presumably due to collisional de-excitation occurring where the density is higher. The [O III]/Hβ ratio is highest (up to 20) in regions of intermediate density, mostly towards the outer parts of the nebula.

clearly visible in an object caught in this brief phase of its evolution. The Hβ luminosity is similar to the intensity observed[7] in 1994 from which it was determined that the luminosity of the entire nebular emission is ~5,000 times the solar luminosity[5] (assuming a distance of 5.6 kpc to the nebula[15,16]).

The dynamics in the Stingray nebula are very complex, as evidenced by a number of additional features that are apparent in the HST images. There are two axes of symmetry: one defined by the bright inner ring, and one defined by the polar holes. The images presented here appear to show that the pairs of collimated, bipolar outflows outside the polar holes have different orientations. The position angles of stellar outflows are sometimes seen to vary monotonically with distance from the central star. One example of this occurs in the young planetary nebula He3-1475 (refs 8, 17, 18). This variation is often explained by monotonic precessional motion or a more chaotic "wobbling"[19,20], perhaps involving a companion object. Depending on when the various outflows originate relative to the precessional cycle, the position angles of the collimated outflows can show some variation. In the Stingray nebula, the position angles of successive outflow features appear to change with distance from the central star. The inner collimated outflows, which have most recently emerged from the polar holes, are displaced in position angle from that of the polar holes by 3° in an anticlockwise direction. The position angles of the more extended (and therefore older) outer collimated outflows appear displaced by 5° clockwise from the position angles of the inner collimated outflows. If the position of the polar holes controlled the direction of these outflows, then the precessional motion must involve the bubbles containing the polar holes.

The WFPCI images[7] did not have sufficient resolution to show a faint companion star embedded in the nebula. But in the higher-resolution images presented here, a companion star is clearly visible. The companion lies 0.4″ from the central star, at a position angle of 60°, and, at magnitude $V = 17.0 \pm 0.2$ as measured from the continuum filter centred at 6,193 Å, is 1.6 mag fainter than the central star. (The central star's magnitude of $V = 15.4$ is quite different from previously published magnitudes partly because the luminosity is dropping, as seen from the comparison of ground-based observations[5,15] between 1985 and 1992, and as expected from the decreasing ultraviolet flux of the central star[5]. Perhaps more importantly, the older, ground-based observations could not resolve the nebula and therefore provided only a combined magnitude of

the star plus the nebula.) The magnitude determination at other wavelengths has higher uncertainty because of the strong nebular emission, but the flux of the companion star is consistent with its being a late-type star at the same distance as the nebula. In considering whether this is truly a companion star, as opposed to a background star, we also made use of the IASG Galaxy Model[21,22] for the location of the Stingray nebula (galactic longitude $l = 331°$, latitude $b = -12°$). At this location, the probability of finding this star so close (0.4″) to the central star is only ~10^{-4}. The probability is further reduced by a factor of ~3 by the additional constraint on its distance as determined from its colour and luminosity. Indeed, other than the central star, no stars this bright are visible anywhere else in the WFPC2 field of view. These considerations leave little doubt that the star is actually a binary companion.

The detection of a binary companion is significant for several reasons. First, the detection of a binary companion is consistent with theoretical expectations. For example, binary nuclei of planetary nebulae should have a double-peaked period distribution, and most should have a period between 30 and 300,000 years[6]. (Below a critical orbital radius, the companion tends to spiral in during a 'common envelope' phase of mass loss. Above the critical orbital radius, mass-loss from the central star causes the orbital radius to increase as the gravitational potential decreases.) The binary nucleus of the Stingray nebula, having a separation of ~2,200 AU, has a period of about 100,000 years—consistent with the theoretical expectations. Second, it has significant implications for the understanding of the early evolution of bipolar structures in planetary nebulae. There are essentially two ways to produce bipolar outflows: one by a density contrast from the pole to the equator[23], and the other by magnetic fields[24]. In the case of the close binaries, the development of a thick disk in the common envelope phase causes a preferentially bipolar ejection of material. In the case of a wide binary, the companion helps by tidally spinning up the envelope[24]. The spin-up of the envelope by a companion also reduces the minimum magnetic field required for magnetic effects to be important. When the binary separation is large, as seen here, the effect of the companion star would, at most, produce some small collimating effects[25] unless, as described above, its orbit has grown larger owing to mass loss. In the latter case, its effect on the shaping of the nebula may have been more profound. The detection of the binary companion in the case of the Stingray nebula supports the proposed connection between binary central stars and asymmetrical planetary nebulae.

In addition to the overall axisymmetric structure that might be attributable to a companion star, there appears to be a distortion near the northern part of the equatorial ring. (See "spur" in Fig. 2.) This is most easily visible in the Hα, Hβ and [O III] images (Fig. 1), where gas from the ring appears to be drawn towards the companion star. The image shows a number of similar wisps of gas throughout the nebula, so the presence of the spur near the companion star could be coincidental. If, however, it is actually caused by the companion star, that would be notable because, although there has been a fair amount of theoretical work on how a companion star could distort a red-giant envelope, decreasing the pole-to-equator density ratio and thereby producing axial symmetry, the spur may be a case of small-scale distortions of a nebula caused by the binary companion.

The electron temperature was derived using the [O III] line intensity ratios (which are insensitive to the electron density). The resulting temperature is of the order of 1.05×10^4 K, which is typical of planetary nebulae. The electron density can be derived from the Hα intensity[26,27] or the [S II] line ratio[5], which give a consistent value of ~10^4 cm^{-3}. Given a distance of 5.6 kpc (refs 15, 16), the approximate radius of the nebula is 0.025 pc. A density of 10^4 cm^{-3} would then imply a nebular mass of 0.015 times the solar mass ($0.015 M_\odot$). There is no strong abundance variation in the nebula as seen from the ratio of the line intensities.
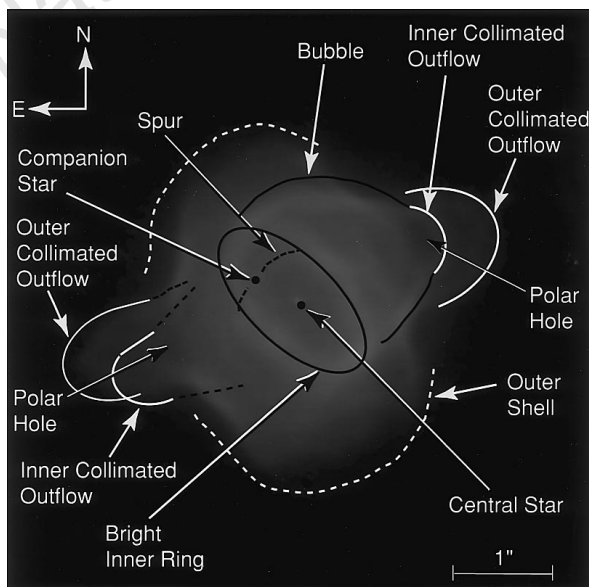

Figure 2 An [O III] 5,007-Å image with various morphological features indicated. See text for details.

A spectrum taken with the International Ultraviolet Explorer (IUE) in 1988 showed[5] a strong P-Cygni profile (an emission feature with a blue-shifted absorption component), suggesting the presence of a fast wind with terminal velocity of $-3,060 \, km \, s^{-1}$. The C IV intensity has since decreased monotonically and had fallen below the detection limit by 1994[28,29]. Our spectrum, taken in 1997, does not show any C IV emission, which confirms that the fast wind has stopped. (The outer shell is the result of the past, slow, red-giant wind.) Because the appearance of multiple collimated outflows implies that the stellar wind is episodic, it is possible that the stellar wind will appear some time again. However, the fact that the ultraviolet flux has also decreased by a factor of 3 within the past eight years[28], combined with the decrease of the C IV emission to an undetectable point now, suggests that the central star has, for now, become devoid of nearby circumstellar material. At the same time, the ionization state of the nebula has increased considerably, which suggests that the temperature of the central star is higher.

The simultaneous drop in the ultraviolet flux and the increase in temperature at this stage imply a drop in the total luminosity of the central star. This places the central star of the Stingray nebula at the "knee" of the Hertzsprung–Russell diagram[30], just before the star evolves towards lower temperatures and lower luminosities. However, these observations reveal some inadequacy in the current theoretical understanding of how these stars evolve. For the central star to evolve as rapidly as observed here, a stellar mass of $0.8 M_\odot$ or more is necessary. However, the luminosity of the central star indicates a core mass of $0.6 M_\odot$ or less, for which the evolution is expected to be much slower than observed[31]. The mass loss in the post-AGB (asymptotic giant branch) stage may be the cause of the unexpectedly rapid evolution and may also cause the differences between observations and theory. The observations clearly show that the central star has become a planetary nebula only within the past few decades[5], and is rapidly evolving to become a DA white dwarf[29]. Although much work on protoplanetary nebulae and other bipolar objects has been done in an attempt to understand the origin of the axial symmetry and collimated outflows, the Stingray nebula shows how far the nebular structure can develop by the time the nebula becomes ionized. We believe that no other planetary nebula in this phase of its evolution has been previously identified. □

1. Kwok, S. in *Late Stages of Stellar Evolution* (eds Kwok, S. & Pottasch, S. R.) 321–335 (Kluwer Academic, Dordrecht, 1987).
2. Maddox, J. Making sense of dwarf-star evolution. *Nature* **376,** 15 (1995).
3. Henize, K. G. Observations of southern planetary nebulae. *Astrophys. J. Suppl. Ser.* **14,** 125–153 (1967).
4. Henize, K. G. Observations of southern emission-line stars. *Astrophys. J. Suppl. Ser.* **30,** 391–550 (1976).
5. Parthasarathy, M. *et al.* SAO 244567: a post-AGB star which has turned into a planetary nebula within the last 40 years. *Astron. Astrophys.* **267,** L19–L22 (1993).
6. Youngelson, L. R., Tutukov, A. V. & Livio, M. The formation of binary and single nuclei of planetary nebulae. *Astrophys. J.* **418,** 794–803 (1993).
7. Bobrowsky, M. Narrowband HST imagery of the young planetary nebula Henize 1357. *Astrophys. J.* **426,** L47–L50 (1994).
8. Borkowski, K. J. *et al.* Collimation of astrophysical jets: the proto-planetary nebula He3-1475. *Astrophys. J.* **482,** L97–L100 (1997).
9. Cantó, J. A stellar wind model for Herbig-Haro objects. *Astron. Astrophys.* **86,** 327–338 (1980).
10. Morris, M. in *From Miras to Planetary Nebulae* (eds Mennessier, M. O. & Omont, A.) 520–535 (Frontières, Gif-sur-Yvette, 1990).
11. Soker, N. & Livio, M. Disks and jets in planetary nebulae. *Astrophys. J.* **421,** 219–224 (1994).
12. Mellema, G. *Astrophys. Space Sci.* **245,** 239–253 (1996).
13. Frank, A. *et al.* A mechanism for the production of jets and ansae in planetary nebulae. *Astrophys. J.* **471,** L53–L56 (1996).
14. Frank, A. & Mellema, G. in *Herbig-Haro Flows and the Birth of Low Mass Stars* (eds Reipurth, B. & Bertout, C.) 291–302 (Kluwer Academic, Dordrecht, 1997).
15. Kozok, J. R. Photometric observations of emission B-stars in the southern Milky Way. *Astron. Astrophys. Suppl. Ser.* **61,** 387–405 (1985).
16. Kozok, J. R. Distances, reddening, and distribution of emission B-stars in the galactic centre region $|l| \leq 45$ deg. *Astron. Astrophys. Suppl. Ser.* **62,** 7–16 (1985).
17. Bobrowsky, M. *et al.* He3-1475 and its jets. *Astrophys. J.* **446,** L89–L92 (1995).
18. Riera, A. *et al.* IRAS 17423-1755 [He3-1475]: a massive post-AGB star evolving into the planetary nebula stage? *Astron. Astrophys.* **302,** 137–153 (1995).
19. Livio, M. & Pringle, J. E. The formation of point-symmetric nebulae. *Astrophys. J.* **465,** L55–L56 (1996).
20. Livio, M. & Pringle, J. E. Wobbling accretion disks, jets, and point-symmetric nebulae. *Astrophys. J.* **486,** 835–839 (1997).
21. Ratnatunga, K. U., Bahcall, J. N. & Casertano, S. Kinematic modeling of the galaxy I. The Yale bright star catalog. *Astrophys. J.* **339,** 106–125 (1989).
22. Casertano, S., Ratnatunga, K. U. & Bahcall, J. N. Kinematic modeling of the galaxy. II. Two samples of high proper motion stars. *Astrophys. J.* **357,** 435–452 (1990).
23. Icke, V., Balick, B. & Frank, A. The hydrodynamics of aspherical planetary nebulae II. Numerical modelling of the early evolution. *Astron. Astrophys.* **253,** 224–243 (1992).
24. Livio, M. HST observations of nebular morphologies and their implications. *Space Sci. Rev.* (in the press).
25. Kolesnik, I. G. & Pilyugin, L. S. The influence of a binary nucleus on the structure of planetary nebulae. *Sov. Astron.* **30,** 169–173 (1986).
26. Sahu, K. C. & Desai, J. N. Kinematic structure of NGC 3132: the planetary nebula with a binary nucleus. *Astron. Astrophys.* **161,** 357–362 (1986).
27. Pottasch, S. R. *Planetary Nebulae* 51–70 (Reidel, Dordrecht, 1983).
28. Parthasarathy, M. *et al.* Fading and variations in the spectrum of the central star of the very young planetary nebula SAO 244567 (Hen 1357). *Astron. Astrophys.* **300,** L25–L28 (1995).
29. Feibelman, W. A. Recent changes in the IUE spectrum of the very young planetary nebula He3-1357 (=SAO 244567). *Astrophys. J.* **443,** 245–248 (1995).
30. Blöcker, T. & Schönberner, D. Stellar evolution of low and intermediate-mass stars. III. An application of evolutionary post-AGB models: the variable central star FG Sagittae. *Astron. Astrophys.* **324,** 991–997 (1997).
31. Blöcker, T. & Schönberner, D. On the fading of massive AGB remnants. *Astron. Astrophys.* **240,** L11–L14 (1990).

Unexpected stellar velocity distribution in the warped Galactic disk

R. L. Smart*, R. Drimmel*, M. G. Lattanzi* & J. J. Binney†

* *Osservatorio Astronomico di Torino, Pino Torinese, TO 10025, Italy*
† *Department of Physics, University of Oxford, Oxford OX1 3NP, UK*

It is now over 40 years since radio observations of neutral hydrogen revealed[1] the gaseous disk of our Galaxy to be warped. Subsequently, the warp has been detected in the distribution of Galactic dust[2], molecular clouds[3], and luminous stars[4,5]. Roughly half of all spiral galaxies have similarly warped disks, which suggests that warps are a common and long-lived phenomenon. However, there is still no consensus as to what induces galactic disks to become warped: intergalactic winds, tidal interactions with satellites, magnetic pressure and massive dark haloes have all been proposed as causative agents. Here we use data from the Hipparcos satellite[6] to determine the small stellar motions in the plane of the sky (proper motions) that should accompany the warp, but which are undetectable in the gas. We find that although the spatial distribution of the stars is in line with previous studies of hydrogen, the velocity distribution has the opposite sign to that expected. Finding a plausible explanation of this result may be the key to solving the long-standing puzzle posed by galactic warps.

A previous attempt to detect warp-induced proper motions[5] was compromised by the difficulty of accurately detecting a small drift across the sky of a large field of stars. Two special features of the Hipparcos results make it possible to detect accurately such motions in this case: (1) its reference frame was set by distant radio galaxies rather than by a dynamical model of the Solar System; and (2) the measurements over the entire celestial sphere were made by a single instrument. Hipparcos proper motions have random errors $\lesssim 1 \, mas \, yr^{-1}$ (ref. 7), accuracies of $\sim 0.1 \, mas \, yr^{-1}$ (ref. 8) and are inertial to better than $0.25 \, mas \, yr^{-1}$ about any axis[7].

To study the kinematics of the warp, we received from the Hipparcos Consortium a sample of 2,422 OB stars with positive parallaxes less than 2 mas, and having a Galactic longitude l in the range (70–290°). OB stars were chosen because they can be seen to large distances, and are young, so presumably trace the warp in the gaseous disk. By selecting stars with small parallaxes, we focus on distant stars and avoid local, small-scale, structure in the OB stellar